10.24425/acs.2020.132584

Archives of Control Sciences
Volume 30(LXVI), 2020
No. 1*, pages 23–45*

A new multi-stable chaotic hyperjerk system, its special features, circuit realization, control and synchronization

VIET-THANH PHAM, SUNDARAPANDIAN VAIDYANATHAN, CHRISTOS VOLOS, SAJAD JAFARI and TOMASZ KAPITANIAK

Researchers have paid significant attention on hyperjerk systems, especial hyperjerk ones with chaos. A new hyperjerk system with seven terms and two parameters is analyzed. Chaotic attractors as well as coexisting attractors are displayed by the hyperjerk system. Thus it is a new multi-stable chaotic hyperjerk system. Further properties of the proposed hyperjerk system such as circuit design and backstepping-based control and synchronization are reported.

Key words: chaos, hyperjerk system, multi-stable, control, synchronization, circuit design

1. Introduction

Studies on chaos theory introduced numerous systems [1–3], interesting properties [4–6]. Chaos theory has several applications like robotics [7], communications [8, 9], oscillators [10–12], memristors [13, 14], biology [15, 16], chemical reactors [17], finance [18], circuits [19], etc.

In the chaos literature, significant attention has been shown in finding chaos in jerk systems [20, 21]. A jerk differential equation in mechanics has a single variable x and a nonlinear function [22]. Therefore, jerk systems are elegant and

V.-T. Pham is with Nonlinear Systems and Applications, Faculty of Electrical and Electronics Engineering, Ton Duc Thang University, Ho Chi Minh City, Vietnam; Division of Dynamics, Lodz University of Technology, Stefanowskiego 1/15, 90-924 Lodz, Poland.

S. Vaidyanathan (Corresponding author), E-mail: sundar@veltech.edu.in, is with School of Electrical and Communication Engineering, Vel Tech University, 400 Feet Outer Ring Road, Vel Nagar, Chennai, India.

C. Volos is with Physics Department, Aristotle University of Thessaloniki, Thessaloniki, Greece.

S. Jafari is with Biomedical Engineering Department, Amirkabir University of Technology, Tehran 15875-4413, Iran.

T. Kapitaniak is with Division of Dynamics, Lodz University of Technology, Stefanowskiego 1/15, 90-924 Lodz, Poland.

This work has been supported by the Polish National Science Centre, MAESTRO Programme-Project No 2013/08/A/ST8/00/780.

Received 2.6.2019. Revised 1.02.2020.

different simple jerk systems were built [23–25]. Recently, Kengne et al. found an autonomous jerk system with multi-stability, which can generate multiple attractors [26]. Multi-stability is a typical feature of nonlinear systems [27–29]. Control and synchronization of jerk systems were also studied [30].

Based on jerk systems, a hyperjerk one is similarly defined [31]. Chaos and hyperchaos were observed in some hyperjerk systems [32, 33, 35]. Bao et al. verified the dependence of memristive hyperjerk type on the initial state of memory element [33]. Vaidyanathan proposed a hyperjerk system with a hyperbolic sinusoidal nonlinear term [34]. Simple hyperjerk one was implemented in Field Programmable Analog Array [35]. Pham et al. found chaos in a simple snap dynamics with just one nonlinear term in a recent work [36].

A novel hyperjerk system with seven terms (only one nonlinear term) is proposed in our work. Its special features such as multi-stability, adjustable size of attractor are presented in Section 2. We introduce its circuit realization in Section 3. We analyze the control applications in Sections 4 and 5. Noticeable conclusions are remarked in Section 6.

2. Features and dynamics of the hyperjerk system

A jerk dynamics [36] is presented by a third order ordinary differential equation:

$$\frac{\mathrm{d}^3x}{\mathrm{d}t^3} = f\left(\frac{\mathrm{d}^2x}{\mathrm{d}t^2}, \frac{\mathrm{d}x}{\mathrm{d}t}, x\right). \tag{1}$$

Researchers attempted to evaluate the extension of jerk system, called hyperjerk [31]:

$$\frac{\mathrm{d}^4x}{\mathrm{d}t^4} = f\left(\frac{\mathrm{d}^3x}{\mathrm{d}t^3}, \frac{\mathrm{d}^2x}{\mathrm{d}t^2}, \frac{\mathrm{d}x}{\mathrm{d}t}, x\right). \tag{2}$$

Motivated by the aforementioned researches, we consider a hyperjerk system in the following form:

$$\frac{\mathrm{d}^4x}{\mathrm{d}t^4} = -\frac{\mathrm{d}^3x}{\mathrm{d}t^3} - \frac{\mathrm{d}x}{\mathrm{d}t} - ax - b\,|x|\,\frac{\mathrm{d}^2x}{\mathrm{d}t^2}. \tag{3}$$

with two positive parameters (a, b).

By denoting

$$y = \frac{\mathrm{d}x}{\mathrm{d}t}, \qquad z = \frac{\mathrm{d}^2x}{\mathrm{d}t^2}, \qquad w = \frac{\mathrm{d}^3x}{\mathrm{d}t^3}, \tag{4}$$

our hyperjerk system is presented in another form:

$$\dot{x} = y, \qquad \dot{y} = z, \qquad \dot{z} = w, \qquad \dot{w} = -ax - y - w - b\,|x|\,z. \tag{5}$$

System (1) shows symmetry via the transformation $(x, y, z, w) \to (-x, -y, -z, -w)$.

The Jacobian matrix of (5) at the unique critical point at the origin $E = (0, 0, 0, 0)$ is represented by

$$J_E = \begin{bmatrix} 0 & 1 & 0 & 0 \\ 0 & 0 & 1 & 0 \\ 0 & 0 & 0 & 1 \\ -a & -1 & 0 & -1 \end{bmatrix}, \tag{6}$$

while the characteristic equation is

$$\lambda^4 + \lambda^3 + \lambda + a = 0. \tag{7}$$

Based on Routh-Hurwitz stability criterion, E is unstable.

We allowed varying the parameter a for $b = 1$ and $X(0) = (0, 0, 0.1, 0)$ and exhibited the bifurcation behavior of the hyperjerk system (5) via Figs. 1 and 2.

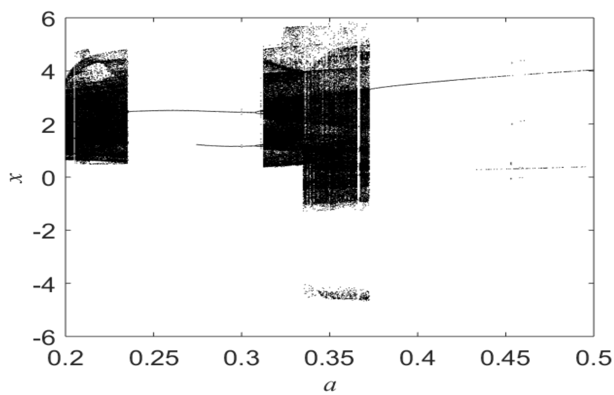

Figure 1: Bifurcation diagram of the hyperjerk system (5)

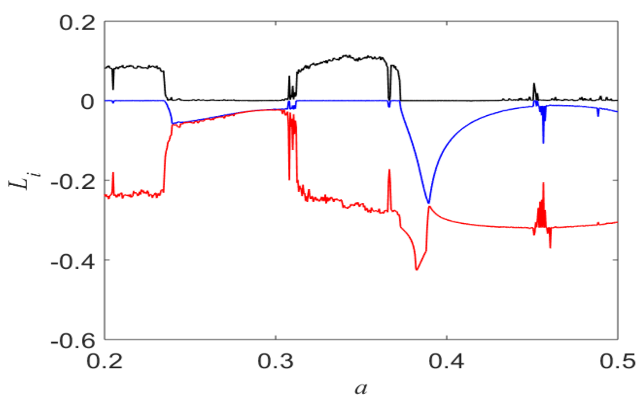

Figure 2: Lyapunov exponents of hyperjerk system (5) for $a \in [0.2, 0.5]$ and $b = 1$ (L_1 (black color), L_2 (blue color) and L_3 (red color))

Interestingly, the system (5) is chaotic in some ranges of a. For example, for $a = 0.35$, $b = 1$, chaotic attractors are shown in Fig. 3, verified by the calculated Lyapunov exponents $L_1 = 0.1036 > 0$, $L_2 = 0$, $L_3 = -0.2563$ and $L_4 = -0.8475$.

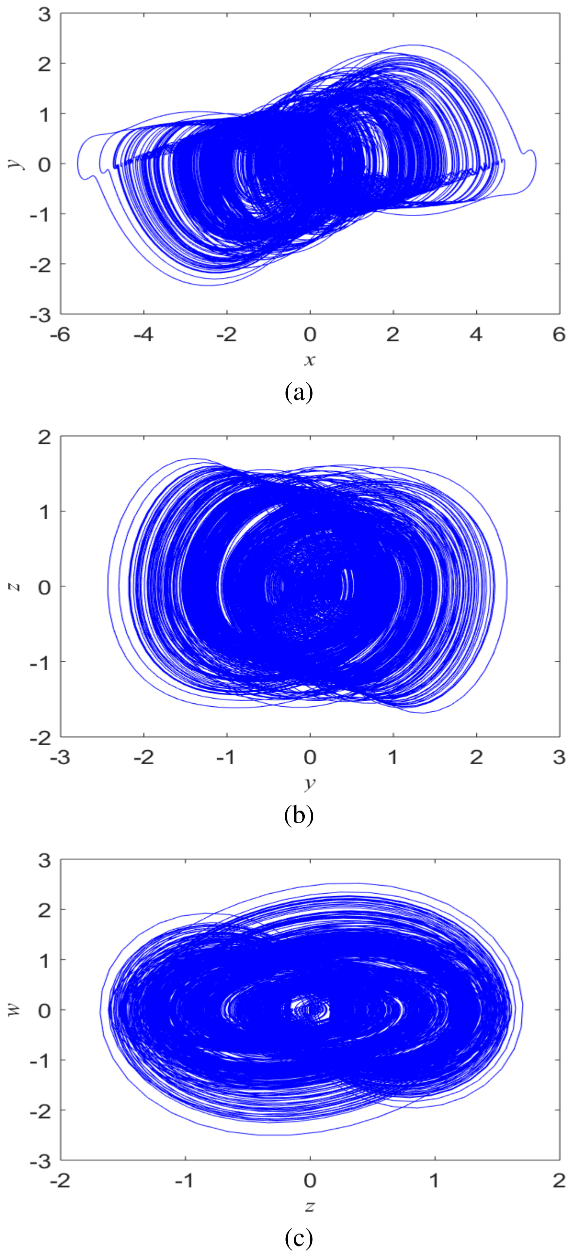

Figure 3: Phase portraits of the hyperjerk system for $(a, b) = (0.35, 1)$ and $X(0) = (0, 0, 0.1, 0)$

It is noted that the hyperjerk system is multi-stable. The coexisting attractors of the chaos hyperjerk dynamics (5) for two initial states $X(0) = (0, 0, 0.1, 0)$ and $X(0) = (0, 0, -0.1, 0)$ are shown in Fig. 4.

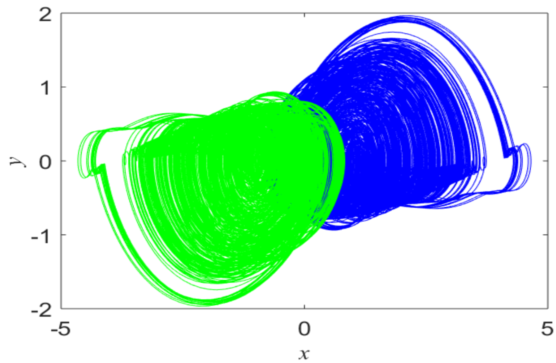

(a)

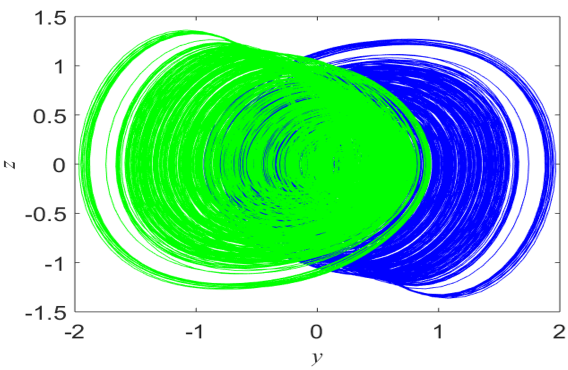

(b)

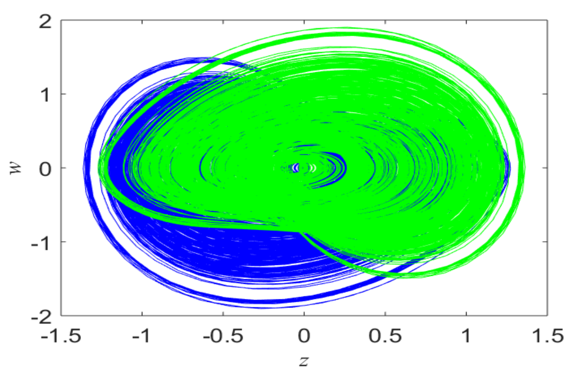

(c)

Figure 4: Coexistence of phase plots in the chaos hyperjerk system (5) for $(a, b) = (0.22, 1)$ when $X(0) = (0, 0, 0.1, 0)$ (blue color) and $X(0) = (0, 0, -0.1, 0)$ (green color)

The parameter b can be seen as a control parameter for changing attractor's size [37–40]. We control the attractor's size by adjusting b as illustrated in Fig. 5.

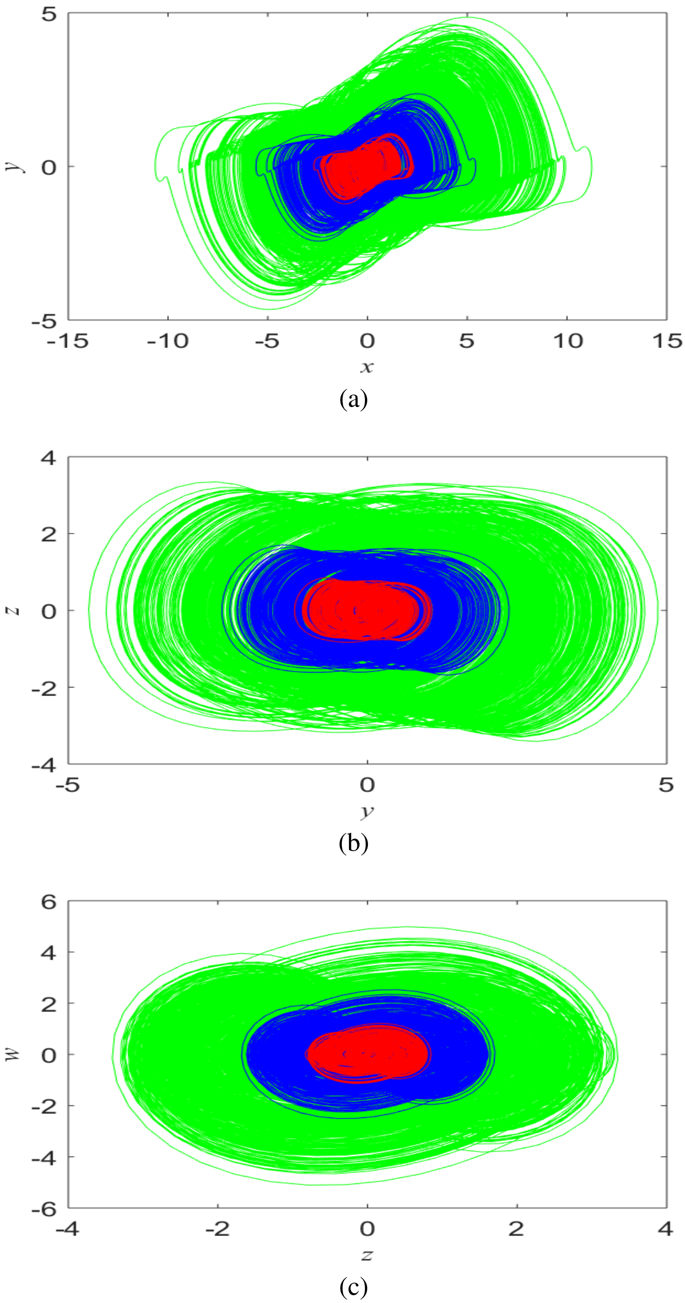

Figure 5: Phase plots of the chaos hyperjerk system (5) for different values of parameter b: b = 0.5 (green color), b = 1 (blue color), b = 2 (red color)

3. Realization of the hyperjerk system

The implementation of mathematical chaos models via hardware tools is of vital importance for practical applications [41, 42].

The schematic of the circuit that emulates system (5) is exhibited in Fig. 6. This circuit has 4 integrators (U_1–U_4), 3 inverting amplifiers (U_5–U_7), which are

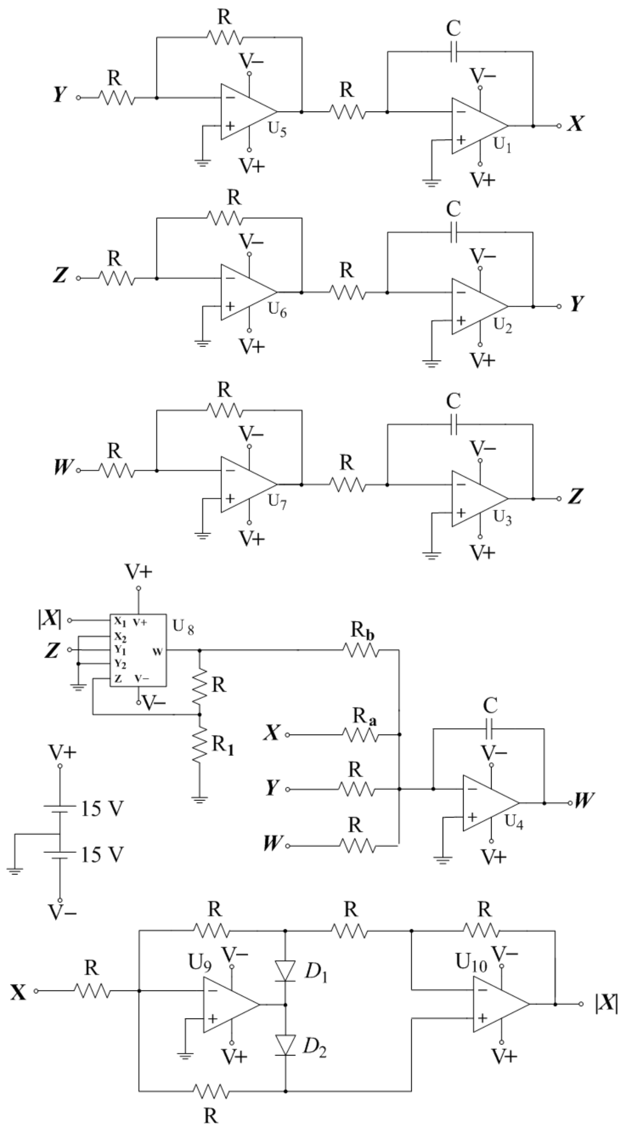

Figure 6: The schematic of the circuit which emulates the proposed chaos hyperjerk system (5)

implemented with the operational amplifier TL084, as well as a signal multiplier (U_8) of type AD633. The last ones (U_9, U_{10}) with the two diodes (1N4007) are used for implementing the absolute function nonlinearity ($|x|$).

The following dynamical system with circuital equations of the designed circuit of Fig. 6 is derived with the help of Kirchhoff's circuit laws.

$$\begin{cases} \dot{X} = \dfrac{1}{RC}Y, \\ \dot{Y} = \dfrac{1}{RC}Z, \\ \dot{Z} = \dfrac{1}{RC}W, \\ \dot{W} = \dfrac{1}{RC}\left(-\dfrac{R}{R_a}X - Y - W - \dfrac{R}{R_b \cdot 1\ \text{V}}\,|X|\,Z\right), \end{cases} \tag{8}$$

where the variables X, Y, Z and W denote the voltages in the outputs of the integrators U_1–U_4.

If we normalize the differential equations of the dynamical system (8) by using $\tau = \dfrac{t}{RC}$, we can observe that this system corresponds to the system (5), with $a = \dfrac{R}{R_a}$ and $b = \dfrac{R}{R_b}$.

The circuit components have been selected as:

$$R = 10\ \text{k}\Omega, \quad R_1 = 90\ \text{k}\Omega, \quad Rb = 10\ \text{k}\Omega, \quad \text{and} \quad C = 10\ \text{nF}.$$

It is noted that the power supplies of all active devices are $\pm 15\ V_{DC}$. For the chosen set of circuit components, the system's parameters are: $b = 1$, while the constant a, represented by the variable resistor R_a plays the role of the control parameter.

The circuit designed in this work has been constructed with the help of common off-the-shelf discrete electronic components on a breadboard as shown in Fig. 7.

For the experimental setup, a digital oscilloscope (HMO1002 of ROHDE & SCHWARZ) has been deployed for observing the measurements and capturing the experimental results.

In this way, the experimental phase portraits of circuit's behavior, for the same values of the parameters a, b as in the corresponding phase portraits of Fig. 3, are depicted as shown in Fig. 8. As expected the obtained experimental results confirm the feasibility of the introduced system (5).

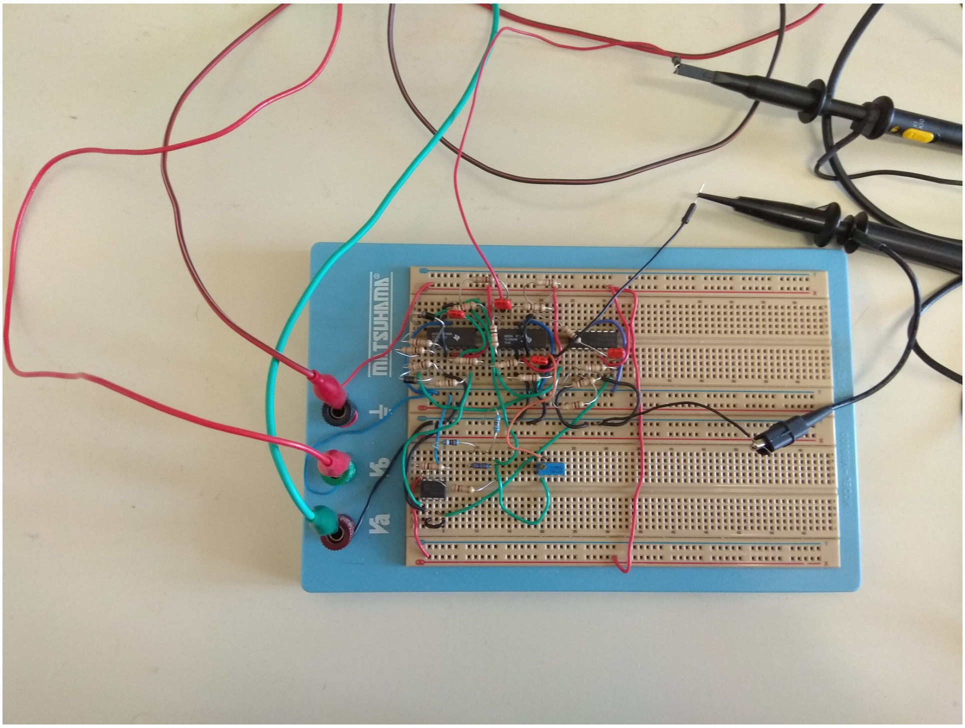

Figure 7: The implementation of the circuit on a breadboard

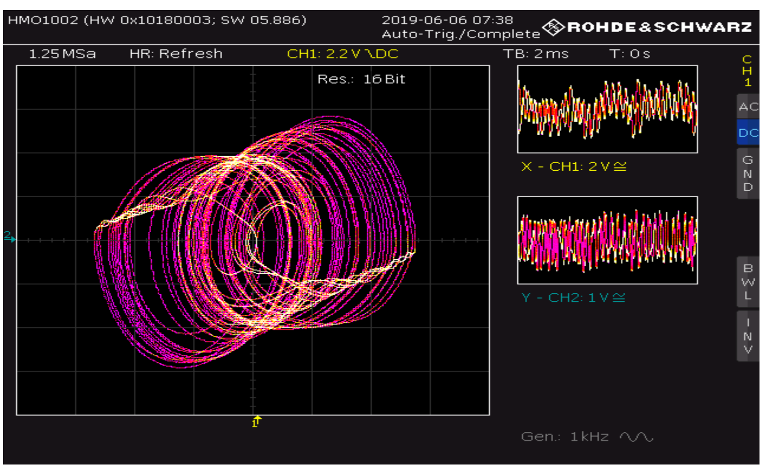

(a)

Figure 8

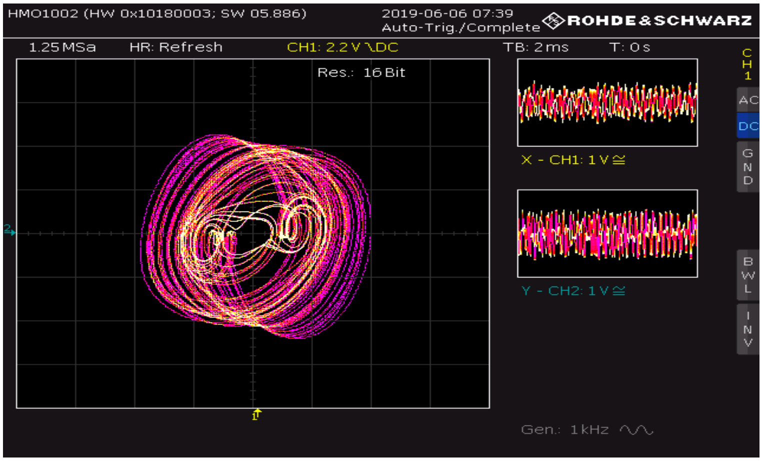

(b)

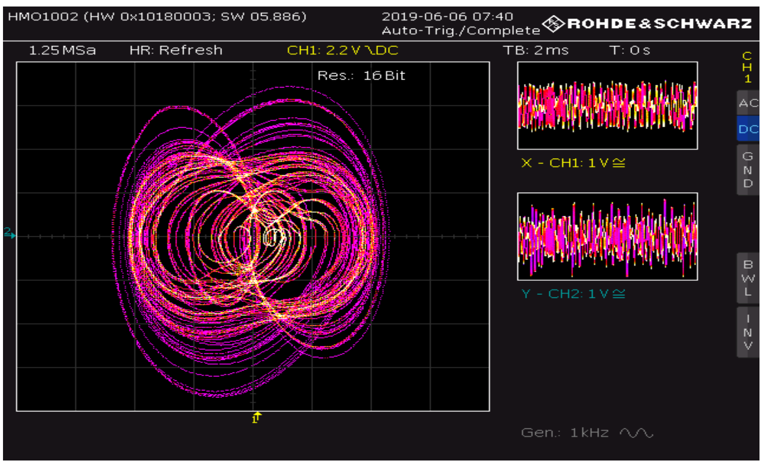

(c)

Figure 8: Experimental phase portraits of circuit's behavior

4. Adaptive control of the new hyperjerk system

We shall deploy adaptive backstepping control here for globally stabilizing the trajectories of the new hyperjerk system for all initial conditions.

The controlled hyperjerk system is described by the 4D dynamics

$$\begin{cases} \dot{x} = y, \\ \dot{y} = z, \\ \dot{z} = w, \\ \dot{w} = -ax - y - w - b|x|z + u. \end{cases} \tag{9}$$

For simplicity in the notation, we define $X = (x, y, z, w)$ as the 4D state of the hyperjerk system (9).

In (9), the values of parameters are unknowns and u is a backstepping control to be determined with the help of $(A(t), B(t))$ that estimates the unknown constants (a, b).

We define

$$\begin{bmatrix} e_a(t) \\ e_b(t) \end{bmatrix} = \begin{bmatrix} a - A(t) \\ b - B(t) \end{bmatrix} \tag{10}$$

which represents the estimation error for the system parameters $(a,\ b)$.

A direct differentiation of the above equation yields

$$\begin{bmatrix} \dot{e_a} \\ \dot{e_a} \end{bmatrix} = \begin{bmatrix} -\dot{A} \\ -\dot{B} \end{bmatrix}. \tag{11}$$

For the control design, we start with the Lyapunov function

$$W_1(\eta_x) = \frac{1}{2}\eta_x^2, \tag{12}$$

where

$$\eta_x = x\,. \tag{13}$$

Differentiating W_1 with respect to t along the hyperjerk system (9), we get

$$\dot{W}_1 = \eta_x\dot{\eta}_x = -\eta_x^2 + \eta_x(x + y). \tag{14}$$

We define

$$\eta_y = x + y\,. \tag{15}$$

With the help of (15), we can express (14) as

$$\dot{W}_1 = -\eta_x^2 + \eta_x\eta_y\,. \tag{16}$$

We proceed next with defining the Lyapunov function

$$W_2(\eta_x, \eta_y) = W_1(\eta_x) + \frac{1}{2}\eta_y^2 = \frac{1}{2}\left(\eta_x^2 + \eta_y^2\right). \tag{17}$$

Differentiating W_2 with respect to t along the hyperjerk system (9), we get

$$\dot{W}_2 = -\eta_x^2 - \eta_y^2 + \eta_y(2x + 2y + z). \tag{18}$$

We define

$$\eta_z = 2x + 2y + z. \tag{19}$$

With the help of (19), we can express (18) as

$$\dot{W}_2 = -\eta_x^2 - \eta_y^2 + \eta_y \eta_z\,. \tag{20}$$

We proceed next with defining the Lyapunov function

$$W_3(\eta_x, \eta_y, \eta_z) = W_2(\eta_x, \eta_y) + \frac{1}{2}\,\eta_z^2 = \frac{1}{2}\left(\eta_x^2 + \eta_y^2 + \eta_z^2\right). \tag{21}$$

Differentiating W_3 with respect to t along the hyperjerk system (9), we get

$$\dot{W}_3 = -\eta_x^2 - \eta_y^2 - \eta_z^2 + \eta_z(3x + 5y + 3z + w). \tag{22}$$

We define

$$\eta_w = 3x + 5y + 3z + w. \tag{23}$$

With the help of (23), we can express (22) as

$$\dot{W}_3 = -\eta_x^2 - \eta_y^2 - \eta_z^2 + \eta_z \eta_w\,. \tag{24}$$

As a final step of the adaptive backstepping control design, we set the quadratic Lyapunov function

$$W(\eta_x, \eta_y, \eta_z, \eta_w) = \frac{1}{2}\left(\eta_x^2 + \eta_y^2 + \eta_z^2 + \eta_w^2\right) + \frac{1}{2}\left(e_a^2 + e_b^2\right). \tag{25}$$

Differentiating W with respect to t along the systems (9) and (11), we get

$$\dot{W} = -\eta_x^2 - \eta_y^2 - \eta_z^2 - \eta_w^2 - e_a\dot{A} - e_b\dot{B} + \eta_w T, \tag{26}$$

where

$$T = \eta_z + \eta_w + \dot{\eta}_w = (5 - a)x + 9y + 9z + 3w - b|x|z + u\,. \tag{27}$$

Theorem 1 *The adaptive backstepping control law stated by*

$$u = -(5 - A(t))x - 9y - 9z - 3w + B(t)|x|z - K\eta_w\,, \tag{28}$$

where $K > 0$ and the parameter estimation law

$$\begin{cases} \dot{A} = -\eta_w x\,, \\ \dot{B} = -\eta_w |x| z \end{cases} \tag{29}$$

with $\eta_w = 3x+5y+3z+w$, globally and asymptotically stabilizes the 4D hyperjerk system (9) for all values of $X(0) \in \mathbf{R}^4$.

Proof. This result is an application of Lyapunov stability theory. First, we remark that the quadratic Lyapunov function W designed via Eq. (25) is positive definite.

Substituting u from Eq. (28) into (27), we get

$$T = -(a - A(t))x - (b - B(t))|x|z - K\eta_w = -e_a x - e_b|x|z - K\eta_w \,. \tag{30}$$

Using (30) and (26), we get

$$\dot{W} = -\eta_x^2 - \eta_y^2 - \eta_z^2 - (1 + K)\eta_w^2 + e_a\left(-\eta_w x - \dot{A}\right) + e_b\left(-\eta_w|x|z - \dot{B}\right). \tag{31}$$

Using the parameter update law (29), the dynamics (31) can be simplified as

$$\dot{W} = -\eta_x^2 - \eta_y^2 - \eta_z^2 - (1 + K)\eta_w^2 \,. \tag{32}$$

From (32), $\dot{W}$ is negative semi-definite on $\mathbf{R}^6$.

Hence, it is deduced via Barbalat's lemma that $(\eta_x(t), \eta_y(t), \eta_z(t), \eta_w(t)) \to 0$ as $t \to \infty$.

Consequently, $(x(t), y(t), z(t), w(t)) \to 0$ as $t \to \infty$ for all $X(0) \in \mathbf{R}^4$. □

For computer simulations, we take $(a, b) = (0.35, 1)$ (chaos case).

We pick $K = 10$, $A(0) = 5$, $B(0) = 4.2$, and $X(0) = (6.5, 1.9, 2.8, 7.5)$.

Figure 9 shows that the backstep-controlled state $X(t) \to 0$ as $t \to \infty$.

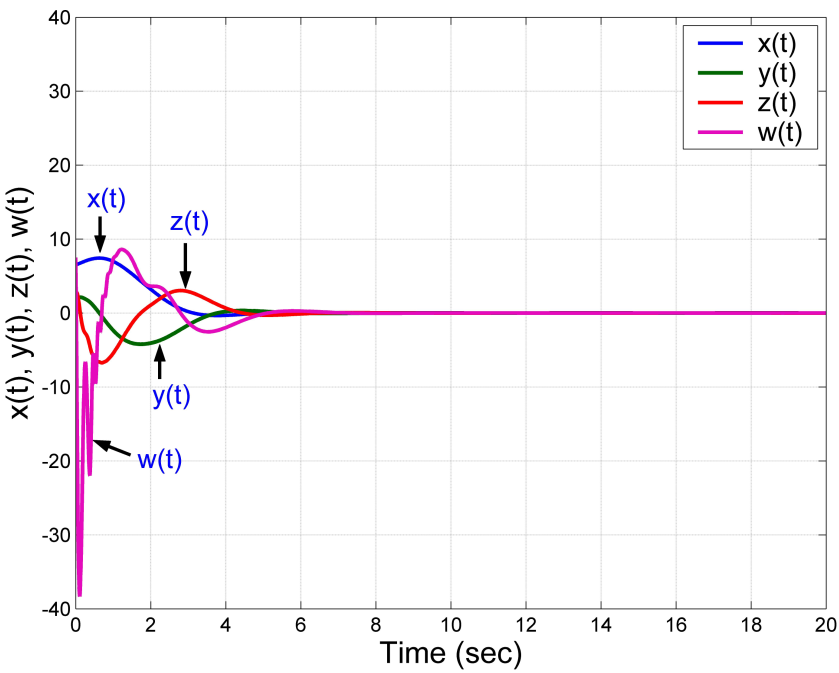

Figure 9: MATLAB plot showing that the states of the chaos hyperjerk system (9) are stabilized asymptotically

5. Adaptive synchronization of the new hyperjerk systems

Here, we shall deploy adaptive backstepping control here for globally synchronizing the trajectories of a set of new chaos hyperjerk systems considered as *leader-follower* systems.

The leader hyperjerk system is taken as the system

$$\begin{cases} \dot{x}_1 = y_1\,, \\ \dot{y}_1 = z_1\,, \\ \dot{z}_1 = w_1\,, \\ \dot{w}_1 = -ax_1 - y_1 - w_1 - b|x_1|z_1\,. \end{cases} \tag{33}$$

For simplicity in the notation, we define $X = (x_1, y_1, z_1, w_1)$ as the 4D state of the hyperjerk system (33).

The follower hyperjerk system is taken as the system

$$\begin{cases} \dot{x}_2 = y_2\,, \\ \dot{y}_2 = z_2\,, \\ \dot{z}_2 = w_2\,, \\ \dot{w}_2 = -ax_2 - y_2 - w_2 - b|x_2|z_2 + u\,. \end{cases} \tag{34}$$

For simplicity in the notation, we define $Y = (x_2, y_2, z_2, w_2)$ as the 4D state of the hyperjerk system (34).

In the leader-follower hyperjerk systems, the values of parameters are unknowns and u is a backstepping control to be determined with the help of $(A(t), B(t))$ that estimates the unknown constants (a, b).

The synchronization chaos error is defined by means of the equations

$$\begin{cases} e_x = x_2 - x_1\,, \\ e_y = y_2 - y_1\,, \\ e_z = z_2 - z_1\,, \\ e_w = w_2 - w_1\,. \end{cases} \tag{35}$$

The synchronization error dynamics is calculated as follows:

$$\begin{cases} \dot{e}_x = e_y\,, \\ \dot{e}_y = e_z\,, \\ \dot{e}_z = e_w\,, \\ \dot{e}_w = -ae_x - e_y - e_w - b(|x_2|z_2 - |x_1|z_1) + u\,. \end{cases} \tag{36}$$

We define

$$\begin{bmatrix} e_a(t) \\ e_b(t) \end{bmatrix} = \begin{bmatrix} a - A(t) \\ b - B(t) \end{bmatrix} \tag{37}$$

which represents the estimation error for the system parameters (a, b).

A direct differentiation of the above equation yields

$$\begin{bmatrix} \dot{e_a} \\ \dot{e_a} \end{bmatrix} = \begin{bmatrix} -\dot{A} \\ -\dot{B} \end{bmatrix}. \tag{38}$$

For the control design, we start with the Lyapunov function

$$W_1(\eta_x) = \frac{1}{2}\,\eta_x^2, \tag{39}$$

where

$$\eta_x = e_x\,. \tag{40}$$

Differentiating W_1 with respect to t along the error system (36), we get

$$\dot{W}_1 = \eta_x\dot{\eta}_x = -\eta_x^2 + \eta_x\left(e_x + e_y\right). \tag{41}$$

We define

$$\eta_y = e_x + e_y\,. \tag{42}$$

With the help of (42), we can express (41) as

$$\dot{W}_1 = -\eta_x^2 + \eta_x\eta_y\,. \tag{43}$$

We proceed next with defining the Lyapunov function

$$W_2(\eta_x, \eta_y) = W_1(\eta_x) + \frac{1}{2}\,\eta_y^2 = \frac{1}{2}\left(\eta_x^2 + \eta_y^2\right). \tag{44}$$

Differentiating W_2 with respect to t along the error system (36), we get

$$\dot{W}_2 = -\eta_x^2 - \eta_y^2 + \eta_y\left(2e_x + 2e_y + e_z\right). \tag{45}$$

We define

$$\eta_z = 2e_x + 2e_y + e_z\,. \tag{46}$$

With the help of (46), we can express (45) as

$$\dot{W}_2 = -\eta_x^2 - \eta_y^2 + \eta_y\eta_z\,. \tag{47}$$

We proceed next with defining the Lyapunov function

$$W_3(\eta_x, \eta_y, \eta_z) = W_2(\eta_x, \eta_y) + \frac{1}{2}\,\eta_z^2 = \frac{1}{2}\left(\eta_x^2 + \eta_y^2 + \eta_z^2\right). \tag{48}$$

Differentiating W_3 with respect to t along the error system (36), we get

$$\dot{W}_3 = -\eta_x^2 - \eta_y^2 - \eta_z^2 + \eta_z \left(3e_x + 5e_y + 3e_z + e_w\right). \tag{49}$$

We define

$$\eta_w = 3e_x + 5e_y + 3e_z + e_w . \tag{50}$$

With the help of (50), we can express (49) as

$$\dot{W}_3 = -\eta_x^2 - \eta_y^2 - \eta_z^2 + \eta_z \eta_w . \tag{51}$$

As a final step of the adaptive backstepping control design, we set the quadratic Lyapunov function

$$W(\eta_x, \eta_y, \eta_z, \eta_w) = \frac{1}{2}\left(\eta_x^2 + \eta_y^2 + \eta_z^2 + \eta_w^2\right) + \frac{1}{2}\left(e_a^2 + e_b^2\right). \tag{52}$$

Differentiating W with respect to t along the systems (36) and (38), we get

$$\dot{W} = -\eta_x^2 - \eta_y^2 - \eta_z^2 - \eta_w^2 - e_a \dot{A} - e_b \dot{B} + \eta_w T , \tag{53}$$

where

$$T = \eta_z + \eta_w + \dot{\eta}_w = (5-a)e_x + 9e_y + 9e_z + 3e_w - b(|x_2|z_2 - |x_1|z_1) + u . \tag{54}$$

Theorem 2 *The adaptive backstepping control law stated by*

$$u = -(5 - A(t))e_x - 9e_y - 9e_z - 3e_w + B(t)\,(|x_2|z_2 - |x_1|z_1) - K\eta_w , \tag{55}$$

where $K > 0$ *and the parameter estimation law*

$$\begin{cases} \dot{A} = -\eta_w e_x , \\ \dot{B} = -\eta_w \,(|x_2|z_2 - |x_1|z_1) \end{cases} \tag{56}$$

with $\eta_w = 3e_x + 5e_y + 3e_z + e_w$*, globally and asymptotically synchronizes the trajectories of the 4D chaos hyperjerk systems (33) and (34) for all values of* $X(0),\ Y(0) \in \mathbf{R}^4$.

Proof. This result is an application of Lyapunov stability theory. First, we remark that the quadratic Lyapunov function W designed via Eq. (52) is positive definite.

Substituting u from Eq. (55) into (54), we get

$$T = -e_a e_x - e_b\,(|x_2|z_2 - |x_1|z_1) - K\eta_w . \tag{57}$$

Using (57) and (53), we get

$$\dot{W} = -\eta_x^2 - \eta_y^2 - \eta_z^2 - (1+K)\eta_w^2 + e_a\left(-\eta_w e_x - \dot{A}\right) + e_b\left[-\eta_w\left(|x_2|z_2 - |x_1|z_1\right) - \dot{B}\right]. \tag{58}$$

Using the parameter update law (56), the dynamics (58) can be simplified as

$$\dot{W} = -\eta_x^2 - \eta_y^2 - \eta_z^2 - (1+K)\eta_w^2\,. \tag{59}$$

From (59), $\dot{W}$ is negative semi-definite on $\mathbf{R}^6$.

Hence, it is deduced via Barbalat's lemma that $(\eta_x(t), \eta_y(t), \eta_z(t), \eta_w(t)) \to 0$ as $t \to \infty$.

Consequently, $(x(t), y(t), z(t), w(t)) \to 0$ as $t \to \infty$ for all $X(0), Y(0) \in \mathbf{R}^4$.

For computer simulations, we take $(a, b) = (0.35, 1)$ (chaos case).

We pick $K = 10$, $A(0) = 4.3$, $B(0) = 5.7$, $X(0) = (3.4, 2.5, 6.8, 1.5)$ and $Y(0) = (1.6, 4.9, 2.1, 8.5)$.

Figures 10–13 shows the synchronization of the chaos hyperjerk systems (33) and (34). Figure 14 shows that the synchronization error $(e_x(t), e_y(t), e_z(t), e_w(t))$ converges to zero as $t \to \infty$.

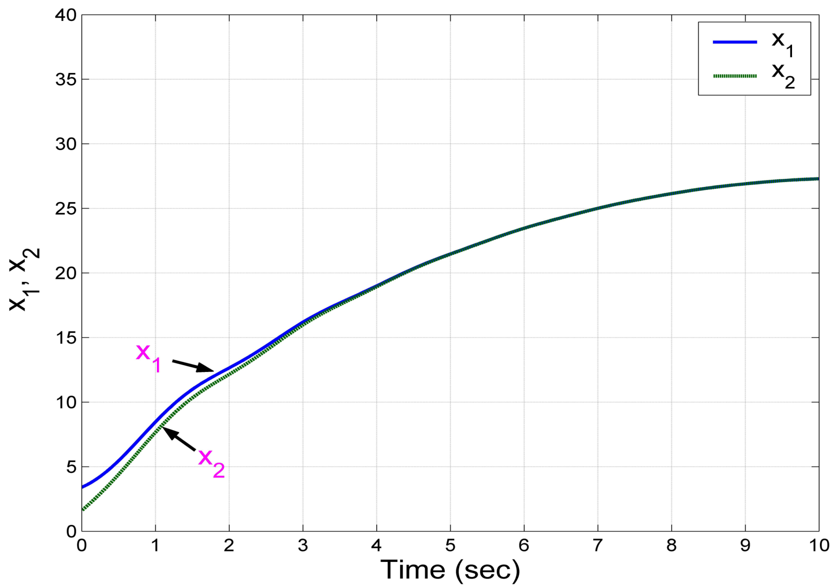

Figure 10: MATLAB plot showing that the signals x_1 and x_2 of the chaos hyperjerk systems (33) and (34) are synchronized asymptotically

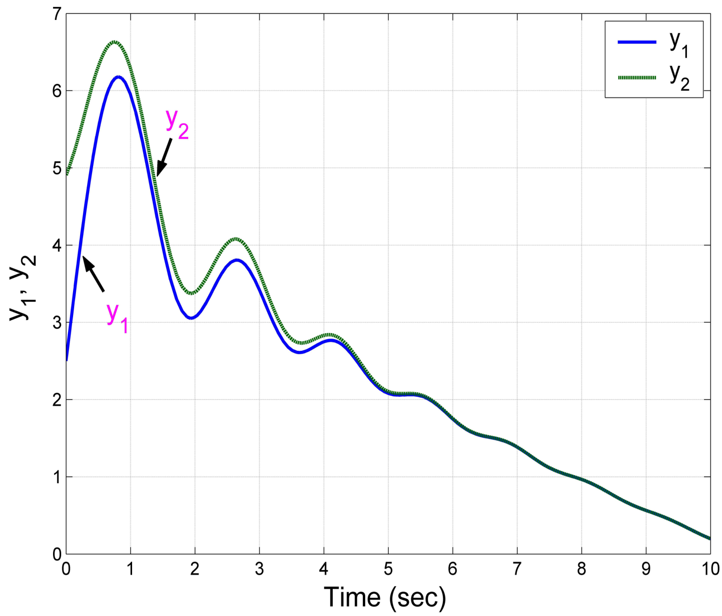

Figure 11: MATLAB plot showing that the signals y_1 and y_2 of the chaos hyperjerk systems (33) and (34) are synchronized asymptotically

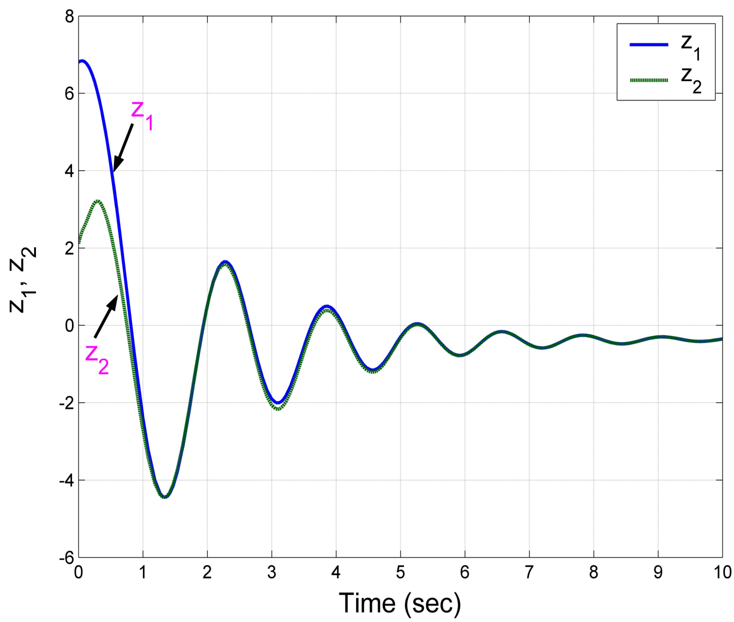

Figure 12: MATLAB plot showing that the signals z_1 and z_2 of the chaos hyperjerk systems (33) and (34) are synchronized asymptotically

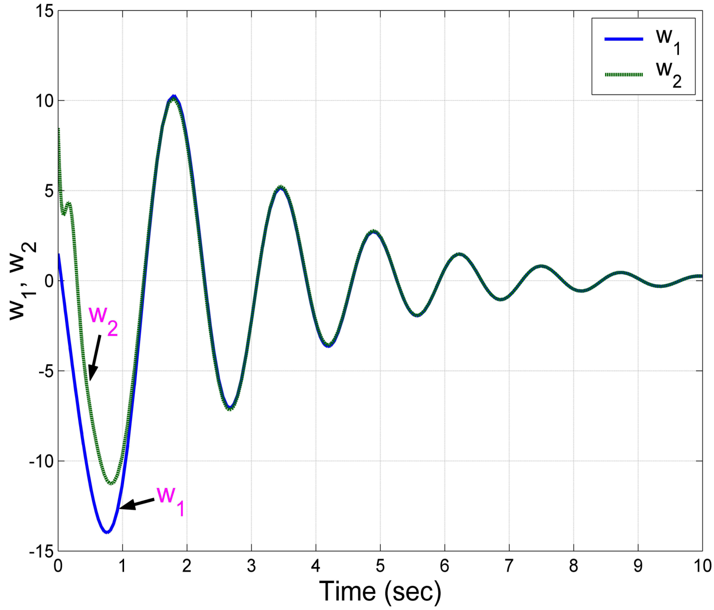

Figure 13: MATLAB plot showing that the signals w_1 and w_2 of the chaos hyperjerk systems (33) and (34) are synchronized asymptotically

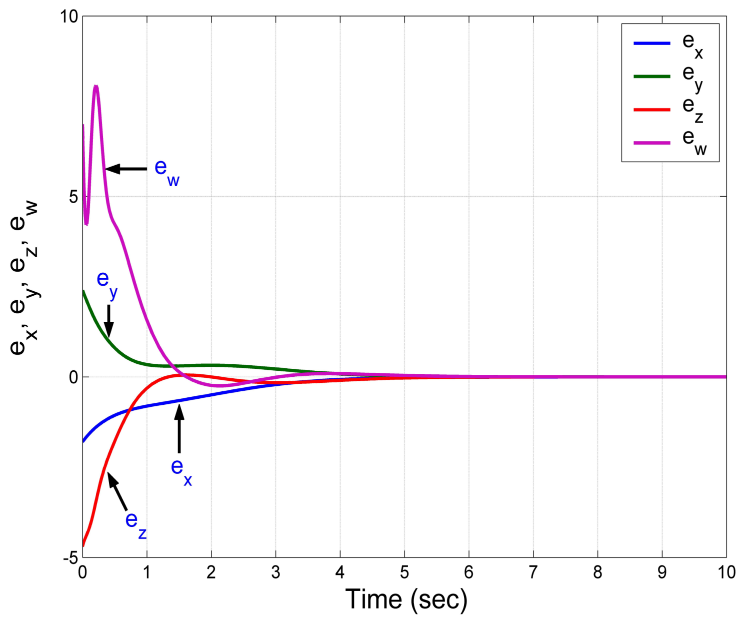

Figure 14: MATLAB plot showing that the synchronization errors between the chaos hyperjerk systems (33) and (34) are stabilized asymptotically

6. Conclusion

By using numerical simulation and circuit design, a hyperjerk system has been studied. Phase portraits and Lyapunov exponents indicate chaos in the system. We have proposed approaches to control and synchronize system's chaos. In our continuing work, extreme behavior in the system will be investigated and application of the system will be developed.

References

[1] S. Behnia, J. Ziaei, and M. Khodavirdizadeh: Detecting a pronounced delocalized state in third-harmonic generation phenomenon; a quantum chaos approach. *Optics Communications*, **416** (2018), 19–24.

[2] V.-T. Pham, C. Volos, S. Jafari, X. Wang, and S. Vaidyanathan: Hidden hyperchaotic attractor in a novel simple memristive neural network, *Optoelectronics and Advanced Materials – Rapid Communications*, **8** (2014), 1157–1163.

[3] S. Vaidyanathan: Synchronization of 3-cells cellular neural network (CNN) attractors via adaptive control method, *International Journal of PharmTech Research*, **8**(5) (2015), 946–955.

[4] S. Vaidyanathan: Global chaos synchronization of the forced Van der Pol chaotic oscillators via adaptive control method, *International Journal of PharmTech Research*, **8**(6) (2015), 156–166.

[5] S. Vaidyanathan and S. Rasappan: Hybrid synchronization of hyperchaotic Qi and Lü systems by nonlinear control, *Communications in Computer and Information Science*, **131** (2011), 585–593.

[6] V.-T. Pham, S. Jafari, C. Volos, and L. Fortuna: Simulation and experimental implementation of a line-equilibrium system without linear term, *Chaos, Solitons and Fractals*, **120** (2019), 213–221.

[7] A. Sambas, S. Vaidyanathan, M. Mamat, W.S.M. Sanjaya and D.S. Rahayu: A 3-D novel jerk chaotic system and its application in secure communication system and mobile robot navigation, *Studies in Computational Intelligence*, **636**, (2016), 283–310.

[8] G.A. Al-Suhail, F.R. Tahir, M.H. Abd, V.-T. Pham, and L. Fortuna: Modelling of long-wave chaotic radar system for anti-stealth applications, *Communications in Nonlinear Science and Numerical Simulation*, **57** (2018), 80–96.

[9] B. Wang, H. Xu, P. Yang, L. Liu, and J. Li: Target detection and ranging through lossy media using chaotic radar, *Entropy*, **17** (2015), 2082–2093.

[10] S. Vaidyanathan: Adaptive control and synchronization design for the Lu-Xiao chaotic system, *Lecture Notes in Electrical Engineering*, **131** (2013), 319–327.

[11] S. Vaidyanathan: Output regulation of the forced Van der Pol chaotic oscillator via adaptive control method, *International Journal of PharmTech Research*, **8**(6) (2015), 106–116.

[12] S. Vaidyanathan: Global chaos synchronization of the forced Van der Pol chaotic oscillators via adaptive control method, *International Journal of PharmTech Research*, **8**(6) (2015), 156–166.

[13] V.T. Pham, S. Vaidyanathan, C.K. Volos, S. Jafari, N.V. Kuznetsov, and T.M. Hoang: A novel memristive time-delay chaotic system without equilibrium points, *European Physical Journal: Special Topics*, **225**(1) (2016), 127–136.

[14] V.T. Pham, S. Jafari, S. Vaidyanathan, C. Volos, and X. Wang: A novel memristive neural network with hidden attractors and its circuitry implementation, *Science China Technological Sciences*, **59**(3) (2016), 358–363.

[15] S. Vaidyanathan: Adaptive control of the FitzHugh-Nagumo chaotic neuron model, *International Journal of PharmTech Research*, **8**(6) (2015), 117–127.

[16] S. Vaidyanathan: Chaos in neurons and adaptive control of Birkhoff-Shaw strange chaotic attractor, *International Journal of PharmTech Research*, **8**(5) (2015), 956–963.

[17] S. Vaidyanathan: Global chaos synchronization of chemical chaotic reactors via novel sliding mode control method, *International Journal of ChemTech Research*, **8**(7) (2015), 209–221.

[18] O.I. Tacha, C.K. Volos, I.M. Kyprianidis, I.N. Stouboulos, S. Vaidyanathan, and V.T. Pham: Analysis, adaptive control and circuit simulation of a novel nonlinear finance system, *Applied Mathematics and Computation*, **276** (2016), 200–217.

[19] V.T. Pham, S. Vaidyanathan, C. Volos, S. Jafari, and S.T. Kingni: A no-equilibrium hyperchaotic system with a cubic nonlinear term, *Optik*, **127** (2016), 3259–3265.

[20] S. Vaidyanathan, C. Volos, V.-T. Pham, K. Madhavan, and B.A. Idowu: Adaptive backstepping control, synchronization and circuit simulation of a 3-D novel jerk chaotic system with two hyperbolic sinusoidal nonlinearities, *Archives of Control Sciences*, **24** (2014), 257–285.

[21] S. Vaidyanathan, A. Sambas, M. Mamat and M. Sanjaya WS: Analysis, synchronisation and circuit implementation of a novel jerk chaotic system and its application for voice encryption, *International Journal of Modelling, Identification and Control*, **28**(2) (2017), 153–166.

[22] S. Schot: Jerk: the time rate of change of acceleration, *American Journal of Physics*, **46** (1978), 1090–1094.

[23] B. Munmuangsaen, B. Srisuchinwong, and J.C. Sprott: Generalization of the simplest autonomous chaotic system, *Physics Letters A*, **375** (2011), 1445–1450.

[24] J.C. Sprott: A new chaotic jerk circuit, *IEEE Transactions on Circuits and Systems-II: Express Briefs*, **58** (2011), 240–243.

[25] K.H. Sun and J.C. Sprott: A simple jerk system with piecewise exponential nonlinearity, *International Journal of Nonlinear Science and Numerical Simulation*, **10** (2009), 1443–1450.

[26] J. Kengne, Z.T. Njitacke, and H. Fotsin: Dynamical analysis of a simple autonomous jerk system with multiple attractors, *Nonlinear Dynamics,* **83** (2016), 751–765.

[27] V.-T. Pham , S. Jafari, C. Volos, and T. Kapitaniak: Coexistence of hidden chaotic attractors in a novel no-equilibrium system, *Nonlinear Dynamics*, **87** (2017), 2001–2010.

[28] V.-T. Pham, C. Volos, S.T. Kingni, T. Kapitaniak, and S. Jafari: Bistable hidden attractors in a novel chaotic system with hyperbolic sine equilibrium, *Circuit, Systems, and Signal Processing*, **37** (2018), 1028–1043.

[29] V.-T. Pham, C. Volos, S. Jafari, and T. Kapitaniak: A novel cubic-equilibrium chaotic system with coexisting hidden attractors: Analysis and circuit implementation, *Journal of Circuits, Systems, and Computers*, **27** (2018), 1850066.

[30] P. Loudopop, M. Kountchou, H. Fotsin and S. Bowong: Practical finite-time synchronization of jerk systems: theory and experiment, *Nonlinear Dynamics*, **78** (2014), 597–607.

[31] K.E. Chlouverakis and J.C. Sprott: Chaotic hyperjerk systems, *Chaos, Solitons & Fractals*, **28** (2006), 739–746.

[32] B. Munmuangsaen and B. Srisuchinwong: Elementary chaotic snap flows, *Chaos, Solitons & Fractals*, **44** (2011), 995–1003.

[33] B. Bao, X. Zou, Z. Liu, and F. Hu: Generalized memory element and chaotic memory system, *International Journal of Bifurcation and Chaos*, **23**(8) (2013), 1350135.

[34] S. Vaidyanathan: Analysis, adaptive control and synchronization of a novel 4-D hyperchaotic hyperjerk system via backstepping control method, *Archives of Control Sciences*, **26**(3), (2016), 311–338.

[35] F.Y. Dalkiran and J.C. Sprott: Simple chaotic hyperjerk system, *International Journal of Bifurcation and Chaos*, **26**(11) (2016), 1650189.

[36] V.-T. Pham, S. Vaidyanathan, C. Volos, S. Jafari, F.E. Alsaadi, and F.E. Alsaadis: Chaos in a simple snap system with only one nonlinearity, its adaptive control and real circuit design, *Archives of Control Sciences*, **29**(1) (2019), 73–96.

[37] C. Li and J.C. Sprott: Amplitude control approach for chaotic signals, *Nonlinear Dynamics*, **73** (2013), 1335–1341.

[38] C. Li and J.C. Sprott: Finding coexisting attractors using amplitude control. *Nonlinear Dynamics*, **78** (2014), 2059–2064.

[39] C. Li and J.C. Sprott: Variable-boostable chaotic flows. *Optik*, **127** (2016), 10389–10398.

[40] V.-T. Pham, A. Akgul, C. Volos, S. Jafari, and T. Kapitaniak: Dynamics and circuit realization of a no-equilibrium chaotic system with a boostable variable, *International Journal of Electronics and Communications*, **78** (2017), 134–140.

[41] L. Fortuna, M. Frasca, and M.G. Xibilia: *Chua's Circuit Implementation: Yesterday, Today and Tomorrow*, World Scientific, Singapore, 2009.

[42] A. Buscarino, L. Fortuna, M. Frasca, and G. Sciuto: *A Concise Guide to Chaotic Electronic Circuits*, Springer, Berlin, Germany, 2014.